

# Cross-Correlation of Instantaneous Phase Increments in Pressure-Flow Fluctuations: Applications to Cerebral Autoregulation

Zhi Chen,<sup>1</sup> Kun Hu,<sup>1,2</sup> H. Eugene Stanley,<sup>1</sup> Vera Novak,<sup>2,\*</sup> and Plamen Ch. Ivanov<sup>1,\*</sup>

<sup>1</sup>*Center for Polymer Studies and Department of Physics,  
Boston University, Boston, Massachusetts 02215, USA*

<sup>2</sup>*Division of Gerontology, Harvard Medical School,  
Beth Israel Deaconess Medical Center, Boston, Massachusetts 02215, USA*

(Dated: June 8, 2021)

We investigate the relationship between the blood flow velocities (BFV) in the middle cerebral arteries and beat-to-beat blood pressure (BP) recorded from a finger in healthy and post-stroke subjects during the quasi-steady state after perturbation for four different physiologic conditions: supine rest, head-up tilt, hyperventilation and CO<sub>2</sub> rebreathing in upright position. To evaluate whether instantaneous BP changes in the steady state are coupled with instantaneous changes in the BFV, we compare dynamical patterns in the instantaneous phases of these signals, obtained from the Hilbert transform, as a function of time. We find that in post-stroke subjects the instantaneous phase increments of BP and BFV exhibit well pronounced patterns that remain stable in time for all four physiologic conditions, while in healthy subjects these patterns are different, less pronounced and more variable. We propose a new approach based on the cross-correlation of the instantaneous phase increments to quantify the coupling between BP and BFV signals. We find that the maximum correlation strength is different for the two groups and for the different conditions. For healthy subjects the amplitude of the cross-correlation between the instantaneous phase increments of BP and BFV is small and attenuates within 3-5 heartbeats. In contrast, for post-stroke subjects, this amplitude is significantly larger and cross-correlations persist up to 20 heartbeats. Further, we show that the instantaneous phase increments of BP and BFV are cross-correlated even within a single heartbeat cycle. We compare the results of our approach with three complementary methods: direct BP-BFV cross-correlation, transfer function analysis and phase synchronization analysis. Our findings provide new insight into the mechanism of cerebral vascular control in healthy subjects, suggesting that this control mechanism may involve rapid adjustments (within a heartbeat) of the cerebral vessels, so that BFV remains steady in response to changes in peripheral BP.

PACS numbers: 05.40.-a,87.19.Hh,87.10.+e

## I. INTRODUCTION

Cerebral autoregulation (CA) is the ability of cerebral blood vessels to maintain steady cerebral perfusion in response to fluctuations of systemic blood pressure (BP), postural changes or metabolic demands. This regulatory mechanism is known to operate over a range of blood pressure values (e.g. 80 - 150 mm Hg) [1] and on time scales of a few heartbeats [2]. The long-term CA compensates for chronic BP elevations and metabolic demands [3]. Ischemic stroke is associated with an impairment of autoregulation [4, 5], that may permanently affect cerebrovascular reactivity to chemical and blood pressure stimuli [6, 7]. With impaired CA, the cerebral blood flow follows BP fluctuations, posing a risk of insufficient blood supply to the brain during transient reductions in peripheral BP. Therefore, evaluating the effectiveness of CA is of great interest, given the clinical implications.

Traditional experimental methods evaluating the mechanism of CA require time-consuming invasive procedures [8, 9] and are focused on long term BP and blood flow velocities (BFV) characteristics such as the mean, lacking descriptors of temporal BP-BFV relationship. To address this problem, an alternative “dynamic” approach has been proposed [10] to quantify CA using transcranial Doppler ultrasound during the transient responses in cerebral BFV to the rapid BP changes induced experimentally by thigh cuff inflation, Valsalva maneuver, tilt-up, or a change in posture [3, 11]. The autoregulation indices derived from this approach may be more sensitive to indicators of hypoperfusion after stroke [12].

The analytic methods evaluating the dynamics of cerebral autoregulation are currently based on mathematical modeling and Fourier transform analysis [13]. The Fourier transform based transfer function method has been widely used [2]. This method estimates the relative cross-spectrum between BP and BFV signals in the frequency domain. Dynamic indices of autoregulation, based on Fourier transform methods, presume (i) signal stationarity (i.e., the mean and standard deviation of the signal are stable and remain invariant under a time shift) and (ii) a linear BP-BFV relationship. However, physiologic signals are often nonstationary reflecting transient responses to physiologic stimuli [14]. The effect of this

---

\*VN and PChI contributed equally to this work. VN designed the clinical study, provided data and guidance of the physiological aspects. PChI proposed the instantaneous phase cross-correlation method, and guided the computational aspects.

nonstationarity on the results obtained from the transfer function analysis has not been carefully assessed in previous studies.

Here we investigate the dynamics of the BP-BFV relationship when the system reaches the quasi-steady state after an initial perturbation. While studies traditionally have focused on the response in BFV to transient changes in BP [3], we hypothesize that spontaneous physiologic fluctuations during the quasi-steady state, which is characterized by absence of physiologic stimuli or constant level of stimulation, may also contain important information about the CA mechanism.

Our focus on fluctuations in the BP and BFV is motivated by previous work which has demonstrated that physiologic fluctuations contain important information about the underlying mechanisms of physiologic control. Robust temporal organization was reported for the fluctuations characterizing cardiac dynamics (inter-beat intervals) [15, 16, 17, 18, 19, 20, 21, 22], respiratory dynamics (inter-breath intervals) [23, 24, 25, 26, 27], locomotion (gait, fore-arm motion) [28, 29, 30, 31, 32, 33], and brain dynamics [34, 35, 36]. Moreover, it has been demonstrated that physiologic fluctuations carry information reflecting the coupling between different physiologic systems, e.g., correlations in the heartbeat change with physical activity [37, 38], with wake and sleep [39], during different sleep stages [40, 41, 42, 43], and even different circadian phases [44]. BP and BFV signals are impacted by the heartbeat, and thus one can expect that fluctuations in BP and BFV may reflect modulation in the underlying mechanisms of control. Previous studies have focused on the transitional changes in BP and BFV in response to abrupt perturbation of the physiologic state, e.g., rapid switch from supine to tilt. In contrast, we focus on the dynamical characteristics of BP and BFV signals after the initial perturbation, when the system has reached a quasi-steady state during which there is no change in physiologic stimuli. Further, we hypothesize that certain dynamical characteristics of the fluctuations in BP and BFV at the steady state, and how these characteristics change for different physiologic conditions, may reflect aspects of the underlying mechanism of CA. For example, under normal CA the fluctuations of the BFV in healthy subjects at the steady state may relate to high frequency adjustments (even within a single heartbeat) of the diameter of the cerebral blood vessels, while loss of CA after stroke may lead to impaired vascular dilation or contraction associated with reduced fluctuations in BFV.

To test this hypothesis, we measure BP and BFV signals from healthy and post-stroke subjects during four physiologic conditions: supine, tilt, hyperventilation, and CO<sub>2</sub> rebreathing in upright position. We apply several complementary methods to quantify the dynamical BP-BFV relationship in these quasi-steady conditions: transfer function analysis, cross-correlation and phase synchronization analyses, and we compare these methods with a *new approach* of cross-correlation between the in-

stantaneous phase increments of BP and BFV signals. Interactions between peripheral circulation (beat-to-beat BP) and cerebral vasoregulation [BFV in the middle cerebral artery (MCA)] can be modeled as dynamic synchronization of two coupled nonlinear systems. Specifically, We hypothesize that the CA mechanism may also involve adjustments in the cerebral vascular tone to spontaneous changes in BP that may be present within a single heartbeat even when the system is in the steady state and there are no significant changes in the mean blood pressure.

The synchronization phenomenon was first observed by Hugenii for two coupled pendulum clocks [45], and since then it has been found in many physical and biological systems where two or more coupled subsystems interact [46, 47, 48, 49, 50, 51, 52]. Alternatively, the synchronization may also be triggered by the influence of external noisy or regular fields [53, 54]. In recent years, the concept of synchronization has been widely used to study the coupling of oscillating systems, leading to the discovery of phase synchronization in non-identical coupled systems in which the instantaneous phases are synchronized, while their instantaneous amplitudes remain uncorrelated [55, 56, 57, 58]. Such phase synchronization has been empirically discovered in a range of physical and physiological systems [59, 60]. Specifically, studies have found coupling between the cardiac rhythm and other systems: phase synchronization was observed between the heartbeat and respiration during normal conditions [61] and during respiratory sinus arrhythmia [62, 63], change of cardiorespiratory phase synchronization with new-borns' age [64] and with the level of anaesthesia [65]. Phase analysis methods have been used to probe spatial synchronization of oscillations in blood distribution systems [66], between cortical centers during migraine [67], as well as between certain brain areas and muscle activity of the limbs [68].

In this study we evaluate the time-domain characteristics of both the amplitudes and the instantaneous phases of the BP and BFV which can be considered as two interacting subsystems within the CA mechanism. To determine the characteristics of the coupling between BP and BFV in healthy subjects and how they change with stroke, we analyze the cross-correlation between the instantaneous phase increments of these two signals. We find that this cross-correlation is much stronger for post-stroke subjects, indicating increased synchronization between BP and BFV, which suggests impaired mechanism of the CA. We compare the results of the instantaneous phase increment cross-correlation analysis with those obtained from several complementary methods including the transfer function, cross-correlation and phase synchronization analyses.

Variable	Demographic characteristics									
	Control					Stroke				
Men/Women	4/7					7/6				
Age(mean±SD)	48.2 ± 8.7					52.8 ± 7.1				
Race W/AA	10/1					12/1				
Stroke side (Right/Left)	-					5/8				
Group (mean±SD)	Supine		Tilt		Hyperventilation		CO <sub>2</sub> rebreathing		Statistics	
	Control	Stroke	Control	Stroke	Control	Stroke	Control	Stroke	(P values)	
BP (mm Hg)	96.4 ± 20.9	101.0 ± 20.6	93.1 ± 20.1	105.9 ± 22.5	94.2 ± 19.7	105.4 ± 22.0	97.6 ± 21.7	108.8 ± 22.7	0.66*	0.0005†
BFV-MCAR/ Normal side(cm/s)	66.0 ± 18.7	55.2 ± 18.0	57.3 ± 18.1	49.7 ± 18.5	40.3 ± 15.7	39.8 ± 14.9	54.7 ± 21.9	56.3 ± 21.5	< 0.0001*	0.77†
BFV-MCAL/ Stroke side(cm/s)	63.5 ± 19.6	51.1 ± 19.0	54.8 ± 17.1	51.5 ± 19.3	40.8 ± 14.9	41.0 ± 17.9	54.6 ± 21.5	57.4 ± 23.3	< 0.0001*	0.008†
CO <sub>2</sub> (mm Hg)	33.5 ± 6.0	37.7 ± 4.9	32.0 ± 3.6	32.5 ± 2.5	21.0 ± 4.5	23.5 ± 8.0	34.6 ± 7.2	33.2 ± 6.5	< 0.0001*	0.28†
CVR**/Normal side	1.54 ± 0.45	1.96 ± 0.54	1.75 ± 0.53	2.28 ± 0.93	2.68 ± 1.10	3.00 ± 1.28	1.97 ± 0.61	2.17 ± 0.83	0.0001*	0.007†
CVR-MCAL/ /Stroke side	1.59 ± 0.56	1.97 ± 0.65	1.79 ± 0.61	2.29 ± 0.83	2.57 ± 0.90	3.04 ± 1.60	1.96 ± 0.56	2.19 ± 0.94	0.0001*	0.01†

\* P value between physiologic conditions comparisons

† P value between groups comparisons

\*\* CVR (cerebral vascular resistance) is defined as mean BP/BFV

TABLE I: Demographic characteristics.

## II. METHODS

### A. Study Groups

We obtain data from the Autonomic Nervous System Laboratory at the Department of Neurology at The Ohio State University and from the SAFE (Syncope and Falls in the Elderly) Laboratory at the Beth Israel Deaconess Medical Center at Harvard Medical School. All subjects have signed informed consent, approved by the Institutional Review Boards. Demographic characteristics are summarized in Table I. Control group: 11 healthy subjects (age  $48.2 \pm 8.7$  years). Stroke group: 13 subjects with a first minor ischemic stroke ( $> 2$  months after acute onset) (age  $52.8 \pm 7.1$  years). Post-stroke subjects have a documented infarct affecting  $< 1/3$  of the vascular territory as determined by MRI or CT with a minor neurological deficit (Modified Rankin Score scale  $< 3$ ). The side of the lesion is determined by neurological evaluation and confirmed with MRI and CT. The lesion is in the right hemisphere in 5 of the subjects and in the left hemisphere in 8 of the subjects. Normal carotid Doppler ultrasound study is required for participation. Patients with hemorrhagic strokes, clinically important cardiac disease including major arrhythmias, diabetes and any other systemic illness are excluded. All subjects are carefully screened with a medical history, physical and laboratory examination.

### B. Experimental Protocol

All subjects have participated in the following experimental protocol:

- Baseline supine rest — normal breathing (normocapnia): subject rests in supine position for 5 minutes on a tilt table;
- Head-up tilt — upright normocapnia: The tilt table is moved upright to an  $80^\circ$  angle. The subject remains in upright position for 5 minutes and is breathing spontaneously;
- Hyperventilation — upright hypocapnia: the subject is asked to breathe rapidly at  $\approx 1$  Hz frequency for 3 minutes in an upright position. Hyperventilation induces hypocapnia (reduced carbon dioxide), which is associated with cerebral vasoconstriction;
- CO<sub>2</sub> rebreathing — upright hypercapnia: The subject is asked to breathe a mixture of air and 5% CO<sub>2</sub> from rebreathing circuit at a comfortable frequency for 3 minutes in an upright position. CO<sub>2</sub> rebreathing increases carbon dioxide above normal levels and induces hypercapnia, which is associated with vasodilatation.

The mechanism of CA is at least partially related to the coupling between metabolic demands and oxygen supply to the brain [3]. Carbon dioxide (CO<sub>2</sub>) is one of the most potent chemical regulators of cerebral vasoreactivity. Head-up tilt provides both pressure and chemical stimulus — BFV and CO<sub>2</sub> decline in upright position, reflecting the change in intracranial pressure and shifting autoregulatory curve towards lower BP values. There is a linear relationship between CO<sub>2</sub> values and cerebral blood flow: hypocapnia (through hyperventilation) causes vasoconstriction and thus decreases

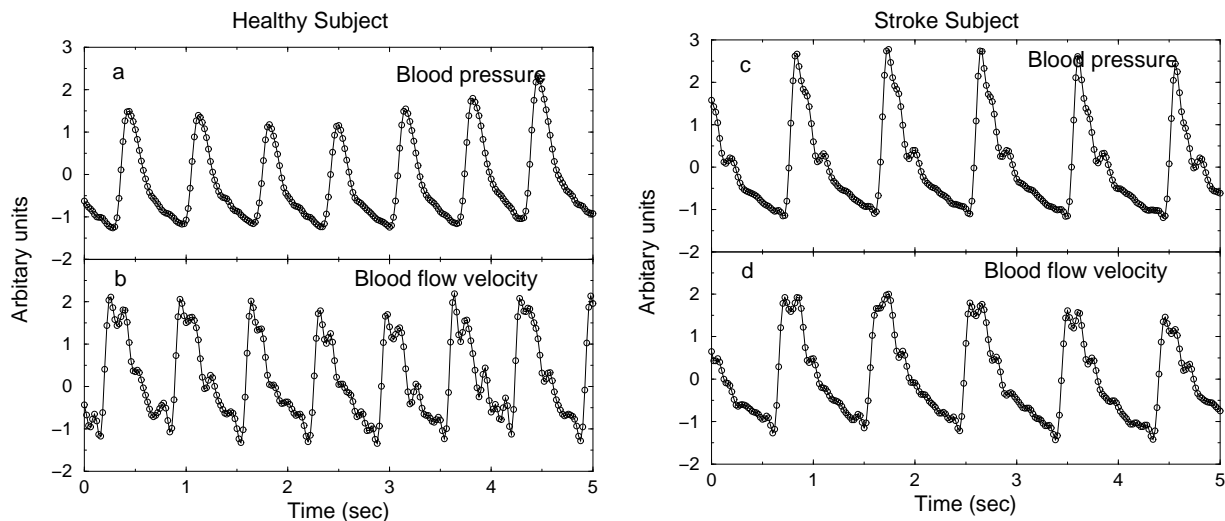


FIG. 1: BP and BFV signals during  $\text{CO}_2$  re-breathing after a band-pass Fourier filter in the range  $[0.05\text{Hz}, 10\text{Hz}]$  and normalization to unit standard deviation: (a-b) for a healthy subject, (c-d) for a post-stroke subject.

the blood flow, hypercapnia (through  $\text{CO}_2$  rebreathing) causes vasodilatation and increases the blood flow in the brain [3].

### C. Data Acquisition

We perform experiments in the morning or more than 2 hours after the last meal. We measure the electrocardiogram from a modified standard lead II or III using a SpaceLab Monitor (SpaceLab Medical Inc., Issaquah, WA). We record beat-to-beat BP from a finger with a Finapres device (Ohmeda Monitoring Systems, Englewood CO), which is based on a photoplethysmographic volume clamp method. During the study protocol, we verify BP by arterial tonometry. With finger position at the heart level and temperature kept constant, the Finapres device can reliably track intraarterial BP changes over prolonged periods of time. We measure the respiratory waveforms with a nasal thermistor. We measure  $\text{CO}_2$  from a mask using an infrared end tidal volume  $\text{CO}_2$  monitor (Datex Ohmeda, Madison WI). We insonate the right and left MCAs from the temporal windows, by placing the 2-MHz probe in the temporal area above the zygomatic arch using a transcranial Doppler ultrasonography system (MultiDop X4, DWL Neuroscan Inc, Sterling, VA). Each probe is positioned to record the maximal BFV and is fixed at a desired angle using a three-dimensional positioning system attached to the light-metal probe holder. Special attention is given to stabilizing the probes, since their steady position is crucial for reliable, continuous BFV recordings. BFV and all cardiovascular analog signals are continuously acquired on a beat-to-beat basis and stored for off-line post-processing. We visually inspect the data and remove occasional extrasystoles and outlier data points using lin-

ear interpolation. We use the Fourier transform of the Doppler shift (the difference between the frequency of the emitted signal and the echo frequency of the reflected signal) to calculate BFV. BFVs in the MCA correlate with invasive measurements of blood flow with xenon clearance, laser Doppler flux and positron emission tomography [69, 70, 71]. Since the MCA diameter is relatively constant under physiological conditions [72], BFV can be used for blood flow estimates.

### D. Statistical Analyses

We use the multiple analysis of variance (MANOVA) with  $2 \times 4$  design for the two groups (control and stroke) and for four physiologic conditions (supine, tilt, hyperventilation, and  $\text{CO}_2$  rebreathing) with subjects as nested random effects (JMP version 5 Software Analysis Package, SAS Institute, Cary, NC). For each group and condition, we calculate: (i) the mean BP, BFV, cerebral vascular resistance (CVR, calculated by mean BP/BFV) from the right and the left MCAs, and  $\text{CO}_2$  (see Table I); (ii) gain, phase and coherence from transfer function analysis (see Table II); and (iii) the direct cross-correlation, the phase synchronization, and the cross-correlation of instantaneous phase increments of BP and BFV (see Table III). We analyze BFV on the stroke side in the right MCA in 5 patients and in the left MCA in 8 patients. In our comparative tests, we consider the side opposite to the stroke side as the “normal” side, as we did not *a priori* know whether the side opposite to the stroke side would exhibit normal or perturbed behavior. In the group comparison, we compare the stroke side BFV for the stroke group to the BFV in the left side MCA for the control group because the majority of post-stroke subjects had stroke on their left side. We note

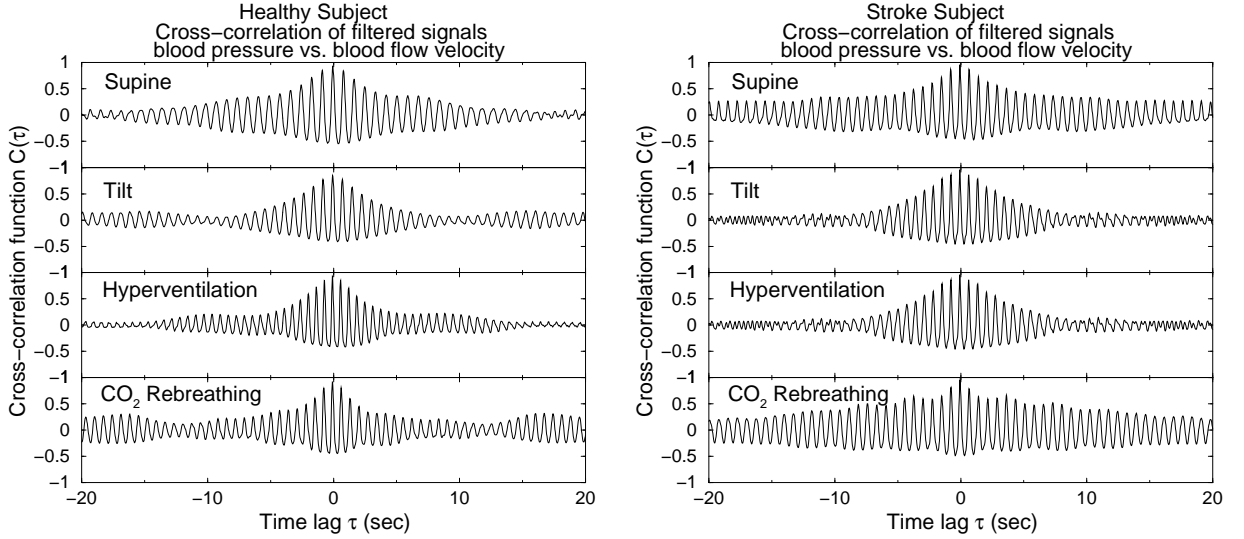


FIG. 2: Cross-correlation function  $C(\tau)$  for the BP and BFV signals during four physiologic conditions: (a) for the same healthy subject and (b) for the same post-stroke subject as shown in Fig. 1. BP and BFV signals are pre-processed using a band-pass Fourier filter in the range [0.05Hz, 10Hz] and are normalized to unit standard deviation before the analysis. Since BFV precedes BP, the maximum value  $C_{\max}$  in the cross-correlation function  $C(\tau)$  is located not at zero lag but at  $\tau \approx -0.1$  sec.

that our comparative tests between the stroke side BFV for post-stroke subjects and the right side BFV for the control group show similar results. We compare the normal side (opposite to the stroke side) BFV for the stroke group to the BFV in the right side MCA for the control group.

#### Method 1: Transfer Function Analysis

We first normalize the BP and BFV signals to unit standard deviation to obtain the respective signals  $P(t)$  and  $V(t)$ . We then calculate their respective Fourier transforms  $V(f)$  and  $P(f)$ . In the frequency domain, the coherence function  $\gamma^2(f)$  is defined as

$$\gamma^2(f) \equiv \frac{|S_{PV}(f)|^2}{S_{PP}(f)S_{VV}(f)}, \quad (1)$$

where  $S_{VV}(f) = |V(f)|^2$ ,  $S_{PP}(f) = |P(f)|^2$  and  $S_{PV}(f) = P^*(f)V(f)$  are the power spectra of  $V(t)$ ,  $P(t)$  and the cross-spectrum of  $V(t)$  and  $P(t)$ , respectively. The value of the coherence function  $\gamma^2(f)$  varies between 0 and 1. The transfer function  $H(f)$  is defined as

$$H(f) \equiv \frac{S_{PV}(f)}{S_{PP}(f)}. \quad (2)$$

From the real part  $H_R(f)$  and imaginary part  $H_I(f)$  of the transfer function, we can obtain its amplitude (also called gain)

$$|H(f)| \equiv [H_R^2(f) + H_I^2(f)]^{1/2}, \quad (3)$$

and its phase

$$\Phi(f) \equiv \arctan[H_I(f)/H_R(f)]. \quad (4)$$

We note that the phase  $\Phi(f)$  is a frequency domain characteristic of the cross-spectrum between two signals, and is different from the instantaneous phase in the time domain we discuss in *Method 3* and *Method 4*.

#### Method 2: Cross-correlation Analysis

To test dynamical aspects of the mechanism of CA, we investigate the cross-correlation between BP and BFV signals and how this cross-correlation changes under stroke. Although we consider segments of the BP and BFV recordings during the quasi-steady state, where we have constant level (or absence) of physiologic stimuli, these signals may still exhibit certain trends in the mean value. So, to eliminate these trends, we first pre-process the BP and BFV signals applying a band-pass filter ( $10\text{Hz} > f > 0.05\text{Hz}$ ) in the frequency domain. To be able to compare signals with different amplitude, we next normalize the band-passed signals to unit standard deviation (Fig. 1). Finally, we perform a cross-correlation analysis estimating the cross-correlation function  $C(\tau)$  for a broad range of values for the time lag  $\tau$ , where  $C(\tau)$  is defined as:

$$C(\tau) \equiv \frac{\langle (P(t) - \langle P \rangle)(V(t + \tau) - \langle V \rangle) \rangle}{\sigma_P \sigma_V}, \quad (5)$$

and  $\langle \dots \rangle$  and  $\sigma$  denote the mean and standard deviation of a signal.

Results of our cross-correlation analysis for one healthy subject and one post-stroke subject during all four physiologic conditions are shown in Fig. 2 and are discussed in Sec. III C.

#### Method 3: Phase Synchronization Analysis

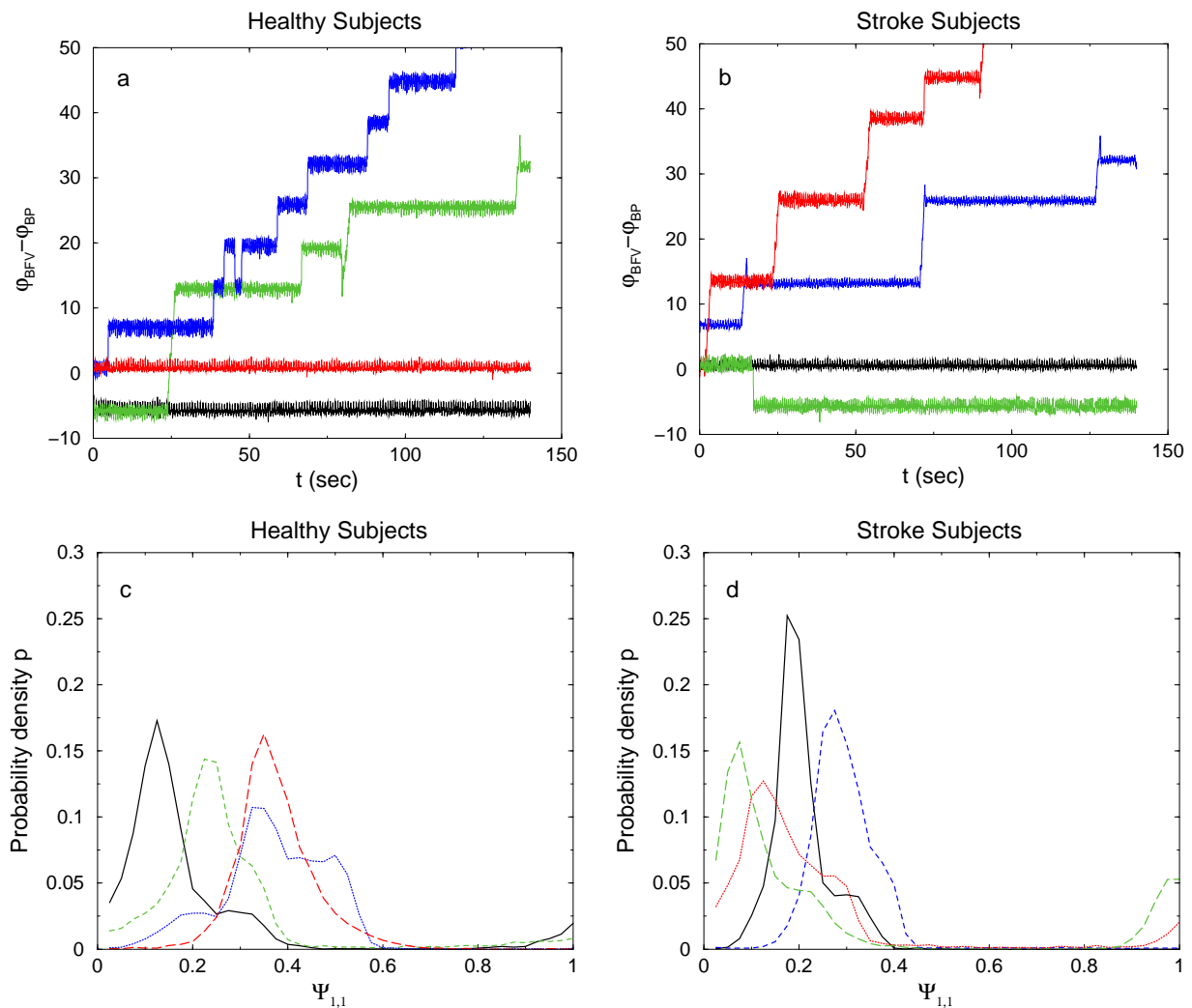


FIG. 3: (a) The relative phases  $\varphi_{BFV}(t) - \varphi_{BP}(t)$  for healthy subjects (a) and post-stroke subjects (b), where  $\varphi(t)$  is the instantaneous phase of a signal. The phase difference of BFV and BP for both groups may fluctuate around a constant value or jump between different constant values. The distributions of  $\Psi_{1,1} \equiv (2\pi)^{-1}[\varphi_{BFV}(t) - \varphi_{BP}(t)] \bmod 1$  for healthy subjects and for post-stroke subjects are shown in (c) and (d), respectively. The number of bins in the histogram is  $N = 40$ .

We study beat-to-beat BP-BFV interaction during quasi-steady state conditions (supine rest, upright tilt, upright hyperventilation and  $\text{CO}_2$  rebreathing employing a phase synchronization method. We first apply a high-pass ( $f > 0.05\text{Hz}$ ) and a low-pass ( $f < 10\text{Hz}$ ) Fourier filter to the BP and BFV signals. The high-pass filter is used to reduce nonstationarity related to slow trends in the mean of the signals. The low-pass filter is used to remove high frequency random fluctuations in the signals. Next we perform the Hilbert transform which for a time series  $s(t)$  is defined as [55, 56, 73, 74, 75, 76]

$$\tilde{s}(t) \equiv \frac{1}{\pi} P \int_{-\infty}^{\infty} \frac{s(\tau)}{t - \tau} d\tau, \quad (6)$$

where  $P$  denotes Cauchy principal value.  $\tilde{s}(t)$  has an apparent physical meaning in Fourier space: for any positive (negative) frequency  $f$ , the Fourier component of

the Hilbert transform  $\tilde{s}(t)$  at this frequency  $f$  can be obtained from the Fourier component of the original signal  $s(t)$  at the same frequency  $f$  after a  $90^\circ$  clockwise (anticlockwise) rotation in the complex plane. For example, if the original signal is  $\sin(\omega t)$ , its Hilbert transform will become  $\cos(\omega t)$ . For any signal  $s(t)$  one can always construct its “analytic signal”  $S$  [55, 56, 73, 74, 76], which is defined as

$$S \equiv s(t) + i\tilde{s}(t) = A(t)e^{i\varphi(t)}, \quad (7)$$

where  $A(t)$  and  $\varphi(t)$  are the instantaneous amplitude and instantaneous phase of  $s(t)$ , respectively. Application of the analytic signal approach to heartbeat dynamics has been shown in [15, 75]. The instantaneous amplitude  $A(t)$  and the instantaneous phase  $\varphi(t)$  are instantaneous characteristics of a time series  $s(t)$ , and present different aspects of the signal. For a pure sinusoid,  $A(t)$  is a con-

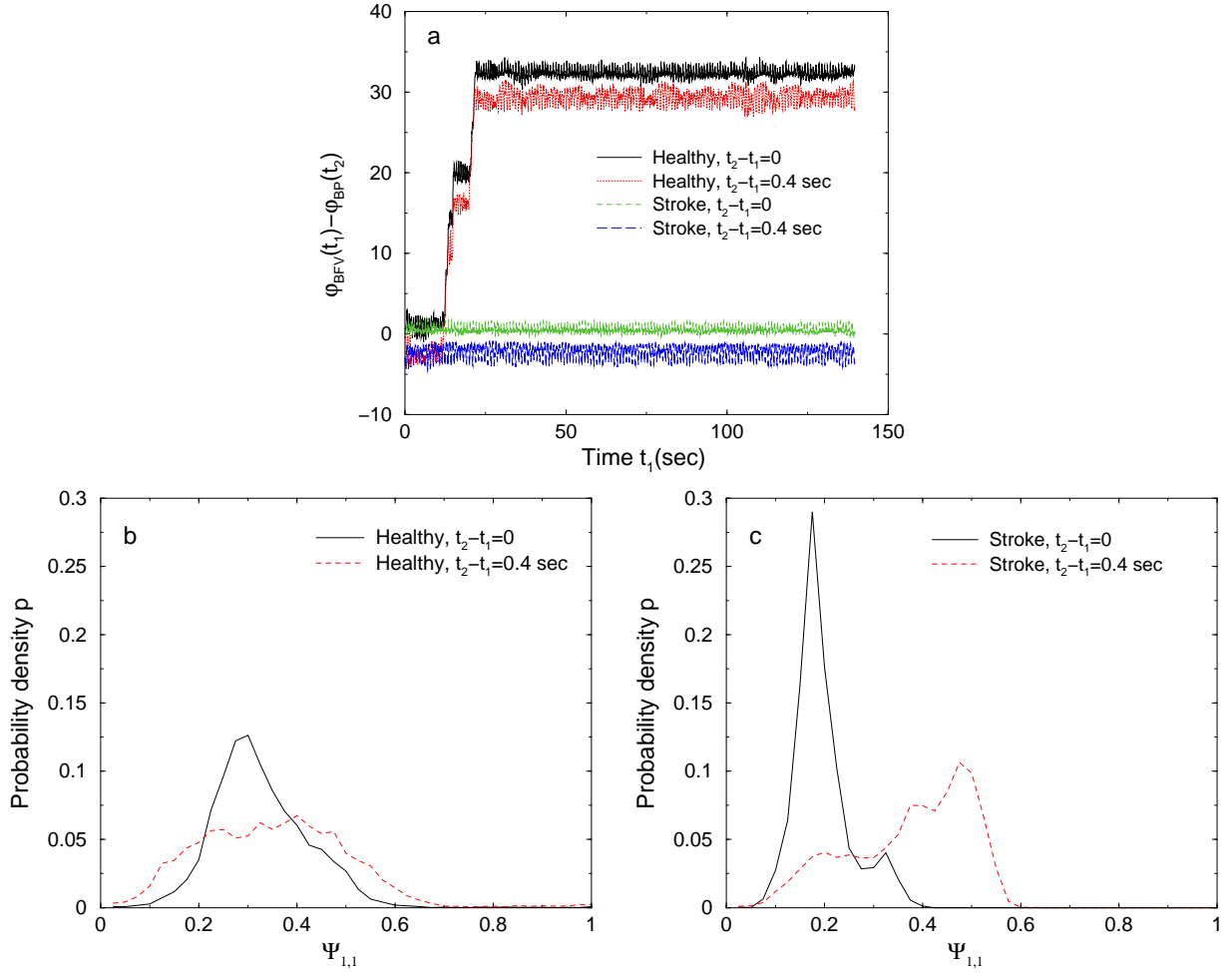


FIG. 4: (a) The relative phases  $\varphi_{BFV}(t_1) - \varphi_{BP}(t_2)$  for a healthy subject and a post-stroke subject. We find that the relative phases between BFV and BP depend on the time difference  $t_2 - t_1$  between these two signals. Accordingly, the distributions of  $\Psi_{1,1} \equiv (2\pi)^{-1}[\varphi_{BFV}(t_1) - \varphi_{BP}(t_2)] \bmod 1$ , shown in (b) and (c) for a healthy subject and a post-stroke subject respectively, also depend on the time difference between BFV and BP. We note that, our choice of time difference  $t_2 - t_1 = 0.4$  sec is arbitrary and does not carry any specific physiologic meaning. The number of bins in the histogram is  $N = 40$ .

stant and  $\varphi(t)$  increases linearly in time: the amplitude quantifies the strength of the oscillation and the slope of the straight line formed by the increasing phase quantifies how fast is the oscillation. For more complex signals, both  $A(t)$  and  $\varphi(t)$  may display complicated forms. Further, we note that the instantaneous phase  $\varphi(t)$  is different from the transfer function phase  $\Phi(f)$ :  $\varphi(t)$  is a time domain characteristic of a single signal, while  $\Phi(f)$  is a cross-spectrum characteristic of two signals in the frequency domain.

From the definition of the Fourier transform one can find that the mean of a given signal  $s(t)$  is proportional to the Fourier component of  $s(t)$  at the frequency  $f = 0$ . After applying the high-pass filter ( $f > 0.05$  Hz), the Fourier component of  $s(t)$  at  $f = 0$  is filtered out, and correspondingly, the mean of the filtered signal becomes zero. Furthermore, from the definition of the Hilbert transform, one can find that the Hilbert transforms of two signals  $s(t)$  and  $s(t) + c$  (where  $c \neq 0$  is a constant)

are identical, although the two original signals have obviously different means due to the constant  $c$ . Since both the instantaneous phase  $\varphi(t)$  and amplitude  $A(t)$  depend on the original signal as well as on the Hilbert transform of the original signal (see Eq. 7), the instantaneous phase and amplitude for  $s(t)$  and  $s(t) + c$  will be also different. However, when we let both signals  $s(t)$  and  $s(t) + c$  pass a high-pass filter ( $f > 0.05$  Hz), the mean of both signals becomes zero, and both signals will have identical phases and amplitudes. Thus, the phase and amplitude of a signal does not depend on its mean, and is uniquely defined after the signal is processed with a high-pass filter.

Following [55] we estimate the difference between the instantaneous phases of the BFV and BP signals  $\varphi_{BFV}(t) - \varphi_{BP}(t)$  at the same time  $t$ . We then obtain the probability density  $p$  for the quantity

$$\Psi_{1,1} \equiv (2\pi)^{-1}[\varphi_{BFV}(t) - \varphi_{BP}(t)] \bmod 1, \quad (8)$$

following the approach presented in [68]. To quantify the

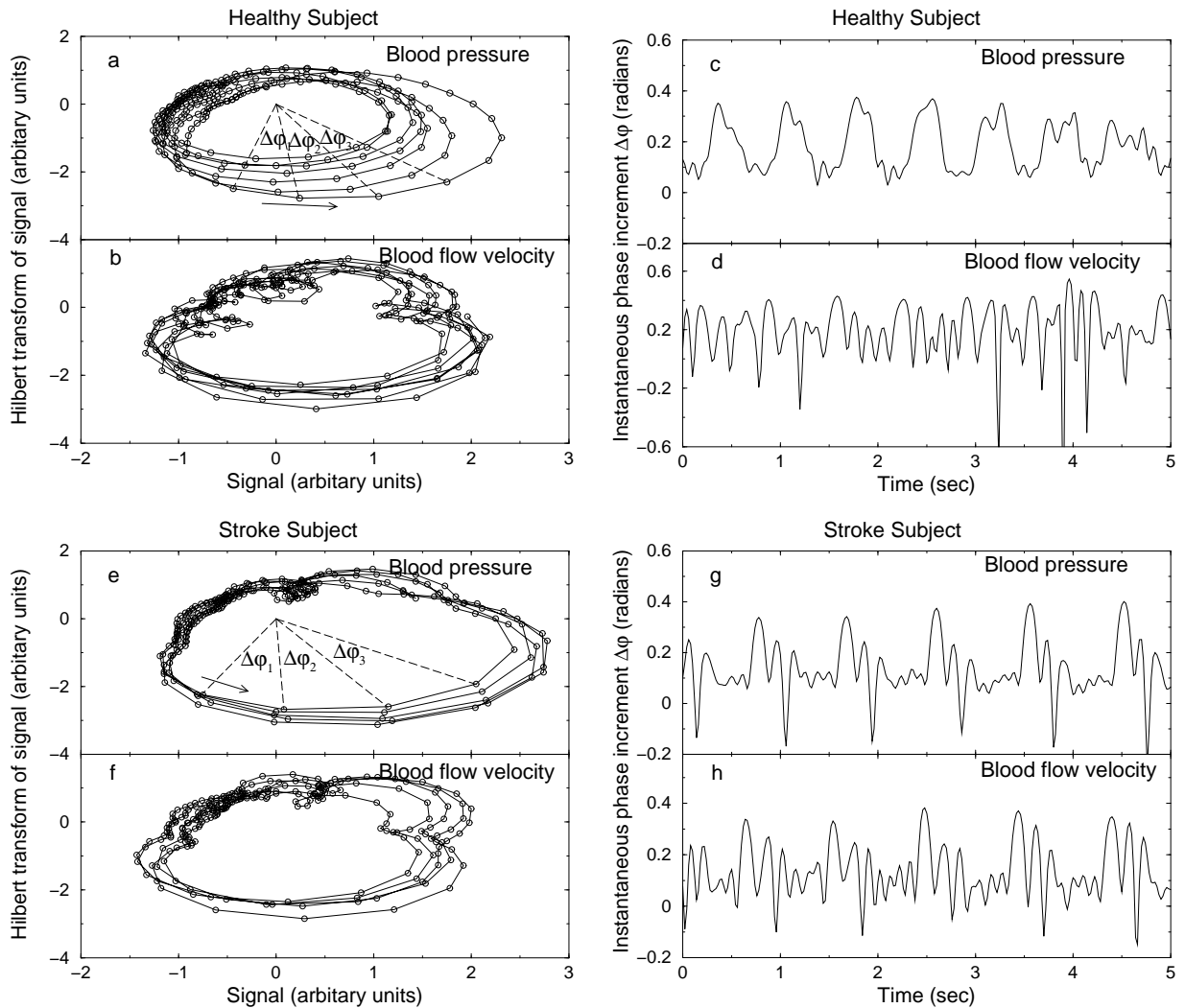


FIG. 5: Presentation of the BP and BFV signals vs. their Hilbert transforms (a-b) and their corresponding instantaneous phase increment  $\Delta\phi$  during the  $\text{CO}_2$  re-breathing condition (c-d) for the same data from a healthy subject as shown in Fig. 1a-b. BP and BFV signals vs. their Hilbert transforms (e-f) and their corresponding instantaneous phase increment  $\Delta\phi$  during the  $\text{CO}_2$  re-breathing condition (g-h) for the same data from a post-stroke subject as shown in Fig. 1c-d. Repetitive temporal patterns associated with each heartbeat in  $\Delta\phi$  for the BP signal from a healthy subject (c) are not matched by corresponding patterns in the BFV signal (d), reflecting active cerebral vascular regulation. In contrast, periodic patterns in  $\Delta\phi$  of the BP signal from a post-stroke subject (g) are matched by practically identical patterns in  $\Delta\phi$  of the BFV signal (h), indicating dramatic impairment of cerebral vascular tone with higher vascular resistance after minor ischemic stroke.

shape of the probability density  $p$ , which can be very broad (uniform) for non-synchronized signals and very narrow (peaked) for strongly synchronized signals, we utilize the index  $\rho$  [68]. The index  $\rho$  is based on the Shannon entropy and is defined as

$$\rho \equiv (S_{\max} - S)/S_{\max}, \quad (9)$$

where  $S = -\sum_{k=1}^N p_k \ln p_k$  is the Shannon entropy of the distribution of  $\Psi_{1,1}$  and  $S_{\max} = \ln N$  corresponds to the uniform distribution, where  $N$  is the number of bins. In our calculations, we choose  $N = 40$ . For the normalized index  $\rho$ , we have  $0 \leq \rho \leq 1$ , where  $\rho = 0$  corresponds to a uniform distribution (no synchronization) and  $\rho = 1$

corresponds to a Dirac-like distribution (perfect synchronization).

Results of our synchronization analysis for several healthy and post-stroke subjects are shown in Figs. 3 and 4, and are discussed in Sec. III D.

#### Method 4: Cross-correlation of Instantaneous Phase Increments

The instantaneous phase  $\varphi(t)$  for both BP and BFV is a nonstationary signal and can be decomposed into two parts: a linear trend and fluctuations along the trend. The trend is mainly driven by the periodic heart rate at a frequency  $\approx 1$  Hz. However, the fluctuations are of specific interest, since they may be affected by the cerebral



autoregulation. To remove the trend, we consider the increments in the consecutive values of the instantaneous phase, defined as

$$\Delta\varphi(t_i) \equiv \varphi(t_i) - \varphi(t_{i-1}), \quad (10)$$

where  $t_i$  and  $t_{i-1}$  are the times corresponding to two successive recordings (in our case we have  $t_i - t_{i-1} = 0.02\text{sec}$ ). The instantaneous phase increment signal  $\Delta\varphi$  is stationary in the sense that it has fixed mean and fixed standard deviation, and fluctuates in the range  $(-\pi, \pi]$ . In Figs. 5(c), 5(d) we show examples of  $\Delta\varphi$  for healthy subjects and in Figs. 5(g), 5(h) for post-stroke subjects.

We then apply a cross-correlation analysis to quantify the dynamical relationship between the stationary phase increments  $\Delta\varphi$  of the BP and BFV signals. For each subject, during each physiologic condition we calculate the correlation coefficient  $C(\tau)$  vs. the time lag  $\tau$  between the BP and BFV signals. To quantitatively distinguish the control group and the stroke group, we further analyze the characteristics of the correlation function  $C(\tau)$ . Specifically, we investigate the maximum value of  $C(\tau)$ , denoted as  $C_{\max}$ , which represents the strength of the cross-correlation between the instantaneous phases of the BP and BFV signals. Another important characteristic of the cross-correlation function is how fast the correlation between two signals decreases for increasing values of the time lag  $\tau$ . To quantify this aspect, we choose a fixed threshold value,  $r = 0.3$ , which is the same for all subjects and for which we obtain a good separation between the control and the stroke group. Since  $C(\tau)$  is a periodic-like function of the time lag  $\tau$  with a decreasing amplitude for increasing  $\tau$  (Fig. 6), we first record all maxima of  $|C(\tau)|$  during each heart beat period ( $\sim 1$  sec), then we determine the two maxima with largest positive and negative time lags  $\tau$  at which the correlation function  $C(\tau)$  is above  $rC_{\max}$ . The average of the absolute values for these two time lags is marked as a characteristic time lag  $\tau_0$ .

In summary we note that, to avoid problems with the nonstationarity when applying the cross-correlation analysis between instantaneous phase increments, we have performed the following steps: (1) We have considered BFV and BP at the steady state for all four physiologic conditions, and we have analyzed only short segments ( $\approx 2.3$  minutes) of data during which the heart rate remains approximately stable; (2) We have performed cross-correlation analysis after pre-processing BFV and BP signals by a high-pass filter, thus removing low frequency trends; (3) The phase increment signals  $\Delta\varphi$  are stationary at least according to the definition of weak stationarity. For the data segments we consider,  $\Delta\varphi$  has a constant mean value and fluctuates within a fixed range  $(-\pi, +\pi]$ .

### III. RESULTS

#### A. Mean Values

We compare the mean values of all signals for both control and stroke groups and for all four physiologic conditions (baseline supine rest, upright tilt, tilt-hyperventilation and  $\text{CO}_2$  rebreathing) using the MANOVA method. Our results are shown in Table I. We see that the mean values of the BFV and  $\text{CO}_2$  signals are significantly different for the four different conditions while the BP mean values are similar. For control and stroke group comparison, we find that BFVs from the left (stroke side) MCA were significantly different, and that the mean value of BP for the stroke group is significantly higher than that for control group. Furthermore, we observe that the cerebral vascular resistance (CVR) is significantly higher for the stroke group.

#### B. Transfer Function Analysis

We apply transfer function analysis on the original BP and BFV signals under different physiologic conditions in both the low frequency (LF) (0.05-0.2 Hz) and the heart beat frequency (HBF) (0.7-1.4 Hz) range. Gain, phase and coherence are calculated for each subject and for all four physiologic conditions (Table II). We use MANOVA to compare our results for the two groups and for the four conditions. In both frequency ranges, we do not find significant difference in the gain. In the LF range, phase  $\Phi(f)$  and coherence  $\gamma^2(f)$  are significantly different between the physiologic conditions, but are not different between the groups. In the HBF range, we find that the phase  $\Phi(f)$  for the MCAL-BFV is significantly different between the conditions ( $p=0.03$ ). The coherence in the HBF range shows no significant difference in the physiologic conditions comparison, however, it is significantly higher for the control group.

#### C. Cross-correlation Analysis

We have performed a cross-correlation analysis directly between the BP and BFV signals, after first pre-processing these signals by a high-pass filter as shown in Fig. 1. Representative examples for the cross-correlation function over a broad range of time lags  $\tau$  for one healthy and one post-stroke subject during the four physiologic conditions (supine, tilt, hyperventilation,  $\text{CO}_2$  rebreathing) are shown in Fig. 2. Group statistics and comparative tests are included in Table III.

The BFV data show more random fluctuations for healthy subjects compared to post-stroke subjects (one example is shown in Fig. 1), leading to slightly reduced cross-correlation amplitude between BP and BFV for healthy subjects. However, the difference in the maximum cross-correlation value  $C_{\max}$  is not significant (see

Frequency Range	Variable		Supine		Tilt		Hyperventilation		CO <sub>2</sub> rebreathing		Statistics	
			BFV-MCAR/ Normal side	BFV-MCAL/ Stroke side	BFV-MCAR/ Normal side	BFV-MCAL/ Stroke side	BFV-MCAR/ Normal side	BFV-MCAL/ Stroke side	BFV-MCAR/ Normal side	BFV-MCAL/ Stroke side	BFV-MCAR/ Normal side	BFV-MCAL/ Stroke side
Low Frequency	Gain	Control	0.94±0.30	0.97±0.27	1.06±0.21	0.97±0.21	0.95±0.41	1.02±0.43	1.03±0.15	1.03±0.15	0.38*	0.11*
	Gain	Stroke	0.84±0.42	0.72±0.37	0.95±0.27	0.95±0.25	1.09±0.36	1.08±0.38	0.92±0.20	0.95±0.21	0.48†	0.26†
0.05-0.2Hz	Coherence	Control	0.65±0.15	0.59±0.21	0.75±0.08	0.66±0.19	0.58±0.18	0.62±0.19	0.82±0.09	0.84±0.08	0.0006*	0.0004*
	Coherence	Stroke	0.53±0.19	0.44±0.24	0.70±0.20	0.66±0.27	0.62±0.17	0.61±0.19	0.69±0.19	0.70±0.20	0.07†	0.07†
	Phase (rad)	Control	0.56±0.27	0.63±0.26	0.62±0.32	0.63±0.30	0.92±0.33	0.94±0.39	0.63±0.23	0.63±0.20	0.0002*	0.0001*
	Phase (rad)	Stroke	0.79±0.27	0.56±0.38	0.58±0.24	0.60±0.25	0.86±0.32	0.94±0.47	0.42±0.25	0.49±0.23	0.74†	0.37†
Heartbeat Frequency	Gain	Control	0.92±0.18	0.93±0.24	0.91±0.15	0.91±0.21	0.88±0.23	0.94±0.23	0.89±0.16	0.91±0.18	0.50*	0.73*
	Gain	Stroke	0.77±0.29	0.82±0.28	0.88±0.27	0.97±0.43	0.97±0.24	0.98±0.28	0.96±0.28	0.97±0.31	0.96†	0.84†
0.7-1.4Hz	Coherence	Control	0.76±0.15	0.75±0.18	0.75±0.13	0.71±0.18	0.58±0.16	0.58±0.18	0.68±0.23	0.70±0.22	0.15*	0.27*
	Coherence	Stroke	0.64±0.24	0.63±0.25	0.57±0.23	0.56±0.21	0.55±0.20	0.56±0.21	0.64±0.25	0.63±0.27	0.035†	0.05†
	Phase (rad)	Control	0.32±0.13	0.27±0.14	0.38±0.18	0.38±0.20	0.46±0.27	0.46±0.26	0.46±0.26	0.42±0.24	0.16*	0.03*
	Phase (rad)	Stroke	0.35±0.31	0.31±0.24	0.36±0.14	0.36±0.21	0.47±0.20	0.49±0.28	0.42±0.21	0.42±0.15	0.95†	0.81†

\* P value between physiologic conditions comparisons

† P value between groups comparisons

TABLE II: Gain, coherence and phase in the low frequency (LF, 0.05-0.2 Hz) range and in the heartbeat frequency (HBF, 0.7-1.4 Hz) range for the control and stroke group during different physiologic conditions. We compare data from BFV in the right MCA (BFV-MCAR) in healthy subjects with data from BFV in the normal side MCA in post-stroke subjects (mean ± standard deviation values are presented in the left column for each condition). We compare data from BFV in the left MCA (BFV-MCAL) in healthy subjects with data from BFV in the stroke side MCA in post-stroke subjects (mean ± standard deviation values are presented in the right column for each condition). The p values from 2x4 MANOVA are calculated for comparing differences between groups and conditions.

Table III), the reason being that the general shape of the BP and BFV oscillations at each heartbeat is very similar for both healthy and post-stroke subjects, and in addition, the amplitude of BP and BFV oscillations is much larger relative to the small random fluctuations on top of these oscillations. In contrast, the shape of the oscillations observed in the phase increments of the BP and BFV signals at every heartbeat is very different for healthy subjects [see Figs. 5(c), 5(d)] but very similar for post-stroke subjects [see Figs. 5(g), 5(h)]. Thus, the instantaneous phase cross-correlation between BP and BFV for healthy subjects is significantly different from post-stroke subjects, as one can see by comparing Fig. 2 and Fig. 6. This difference is also shown in Table III. The comparative statistical tests indicate significant difference between the control and stroke group based on the instantaneous phase cross-correlation parameter  $C_{\max}$  when we compare both the stroke side and the normal side of post-stroke subjects with healthy subjects. There is no significant difference in  $C_{\max}$  obtained from the direct cross-correlation between BP and BFV signals when we compare the normal side of post-stroke subjects with healthy subjects (see also results in Sec. III E).

We also note that, healthy subjects exhibit higher variability in the intervals between consecutive heartbeats, leading to higher variability in the intervals between consecutive peaks in the BP and BFV waves (Fig. 1). As a result, both the direct cross-correlation and the instantaneous phase cross-correlation between the BP and BFV signals decay faster with increasing the time lag  $\tau$  for healthy subjects compared to post-stroke subjects. For

both methods we show that the parameter  $\tau_0$ , which characterizes the decay in the cross-correlations, separates equally well the stroke group from the control group (see Table III).

#### D. Phase Synchronization Analysis

In Fig. 3 we present the results of the phase synchronization analysis for four healthy and four post-stroke subjects. The statistics for all four physiologic conditions (supine rest, tilt, hyperventilation, CO<sub>2</sub> rebreathing) in our database and over the entire control and stroke groups are summarized in Table III. We find a statistically significant difference between the control and stroke group based on the entropy index  $\rho$ .

In the phase synchronization method one estimates the difference between the instantaneous phases of two signals *at the same time*. Thus, the phase synchronization method does not reflect possible time delays between the two studied signals, and correspondingly, between their instantaneous phases. Such time delays can often be observed in coupled physical and physiological systems [51, 77]. To demonstrate the effect of such time delay in context of the system we study, we consider the difference between the instantaneous phases of BP and BFV, when the phase of BFV is taken at time  $t_1$  and the phase of BP is taken at time  $t_2 = t_1 + \tau$ . As we show in Fig. 4, the result of the phase synchronization analysis is very different when considering instantaneous phase difference with a time delay — the histogram of the phase

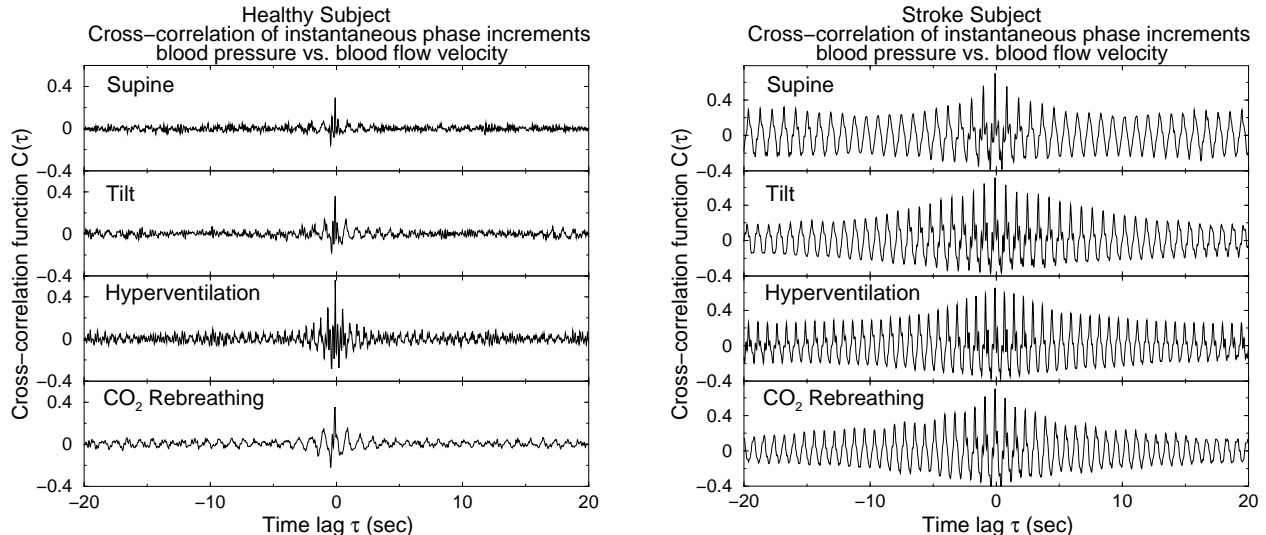


FIG. 6: Cross-correlation function  $C(\tau)$  of the instantaneous phase increment  $\Delta\varphi$  for the BP and BFV signals during four physiologic conditions. We find that the cross-correlation function for all healthy subjects exhibits a very distinct type of behavior compared to post-stroke subjects. Two typical examples are shown. (Left) A healthy subject:  $C(\tau)$  has a small amplitude at  $\tau = 0$  and is close to zero at time lags  $\tau > 5$  seconds during all four conditions. (Right) A post-stroke subject:  $C(\tau)$  has a much larger amplitude at  $\tau = 0$  which lasts for lags  $\tau$  up to 20 seconds, indicating a strong coupling between the BP and BFV signals, i.e., loss of cerebral autoregulation.

difference becomes much broader (the entropy index  $\rho$  much smaller) compared to the case when no time delay is introduced.

Statistics for the groups and physiologic conditions are presented in Table III, and indicate a very different result — no statistically significant difference between the control and stroke group for the entropy index  $\rho$  estimated for an arbitrary chosen time delay of  $\tau = 0.4$  seconds. This is in contrast to the results obtained for the entropy index  $\rho$  from the synchronization analysis when one does not consider a time delay. Thus, the results of the traditional phase synchronization method strongly depend on the time at which the instantaneous phases of two signals are compared [51, 77]. This motivates our approach to investigate the cross-correlation between the instantaneous phases of two coupled systems at different time lag  $\tau$ , as presented in Sec. III E.

### E. Cross-correlation of Instantaneous Phase Increments

We apply the instantaneous phase increments cross-correlation analysis to all four conditions and both study groups. We find that the patterns of the cross-correlation function  $C(\tau)$  of the instantaneous phase increments  $\Delta\varphi$  of the BP and BFV signals are very different for the stroke group compared to the control group. In general, the cross-correlation function  $C(\tau)$  for the control group is characterized by smaller amplitude and faster decay (time lag  $\tau$  less than 10 seconds) [Fig. 6]. In contrast, for post-stroke subjects, the amplitude of the

cross-correlation function  $C(\tau)$  is much larger and decays much slower (over time lags larger than 10 seconds) [Fig. 6]. Thus for those post-stroke subjects the changes of the phase of BFV will change in the approximately same way with that of BP signals, indicating a strong synchronization.

The correlations at short time scales (less than 10 seconds) may be partially attributed to the effect of heart rate ( $\sim 1$  sec) and respiration ( $\sim 5$  seconds)— i.e., they reflect the effect of other body regulations (similar to “background noise”) on both BP and BFV signals. When cerebral autoregulation is effective, because of its fast-acting mechanism [3], it may also contribute to the significantly weaker cross-correlations at short time scales we find in healthy subjects compared to post-stroke subjects (Fig. 6). However, the correlation due to the above mechanisms will decrease very fast when increasing the time lag  $\tau$  between BP and BFV signals. Thus, the correlations at long time scales ( $>10$  seconds) observed for post-stroke subjects (Fig. 6), cannot be attributed to the effect of cerebral autoregulation. Instead, the existence of such strong and sustained cross-correlations may imply that BFV will passively follow the changes of BP, thus indicating absence of vascular dilation or constriction and impaired cerebral autoregulation for the post-stroke subjects.

To quantitatively distinguish the control group from the stroke group, we study the characteristics of the correlation function  $C(\tau)$  for all subjects. For each correlation function  $C(\tau)$ , we first find  $C_{\max}$ , the maximal value of  $C(\tau)$ , which tells the strength of the correlation. Then we choose a threshold value, e.g.,  $r = 0.3$ , search for the

Variable		Supine		Tilt		Hyperventilation		CO <sub>2</sub> rebreathing		Statistics	
		BFV-MCAR/ Normal side	BFV-MCAL/ Stroke side	BFV-MCAR/ Normal side	BFV-MCAL/ Stroke side	BFV-MCAR/ Normal side	BFV-MCAL/ Stroke side	BFV-MCAR/ Normal side	BFV-MCAL/ Stroke side	BFV-MCAR/ Normal side	BFV-MCAL/ Stroke side
direct cross-correl. $C_{\max}$	Control	0.91 ± 0.02	0.89 ± 0.06	0.88 ± 0.05	0.84 ± 0.06	0.88 ± 0.13	0.87 ± 0.12	0.91 ± 0.03	0.91 ± 0.03	0.066*	0.069*
	Stroke	0.92 ± 0.03	0.92 ± 0.03	0.88 ± 0.09	0.89 ± 0.06	0.91 ± 0.06	0.90 ± 0.09	0.92 ± 0.04	0.93 ± 0.04	0.33 <sup>†</sup>	0.024 <sup>†</sup>
direct cross-correl. $\tau_0$	Control	6.5 ± 4.1	6.6 ± 4.1	3.3 ± 1.4	3.5 ± 1.3	3.2 ± 1.2	3.2 ± 1.3	4.8 ± 3.2	5.0 ± 3.4	0.008*	0.01*
	Stroke	11.4 ± 6.6	11.2 ± 6.9	6.5 ± 5.6	6.4 ± 5.6	6.2 ± 5.8	6.2 ± 5.7	9.8 ± 7.2	9.6 ± 7.2	0.0001 <sup>†</sup>	0.0004 <sup>†</sup>
phase synch. index $\rho$ for $\tau = 0$	Control	0.32 ± 0.07	0.31 ± 0.06	0.25 ± 0.07	0.23 ± 0.07	0.21 ± 0.08	0.20 ± 0.08	0.27 ± 0.06	0.26 ± 0.06	< 0.0001*	0.0002*
	Stroke	0.35 ± 0.07	0.34 ± 0.07	0.26 ± 0.09	0.27 ± 0.09	0.25 ± 0.09	0.25 ± 0.10	0.32 ± 0.09	0.32 ± 0.09	0.047 <sup>†</sup>	0.008 <sup>†</sup>
phase synch. index $\rho$ for $\tau = 0.4s$	Control	0.18 ± 0.05	0.17 ± 0.05	0.11 ± 0.05	0.11 ± 0.06	0.11 ± 0.06	0.11 ± 0.06	0.12 ± 0.05	0.12 ± 0.04	< 0.0001*	< 0.0001*
	Stroke	0.21 ± 0.05	0.21 ± 0.05	0.11 ± 0.05	0.12 ± 0.06	0.11 ± 0.06	0.11 ± 0.06	0.13 ± 0.05	0.13 ± 0.05	0.43 <sup>†</sup>	0.18 <sup>†</sup>
phase cross-correl. $C_{\max}$	Control	0.55 ± 0.17	0.49 ± 0.22	0.39 ± 0.16	0.33 ± 0.17	0.47 ± 0.17	0.43 ± 0.16	0.45 ± 0.13	0.41 ± 0.13	0.006*	0.07*
	Stroke	0.62 ± 0.12	0.58 ± 0.14	0.43 ± 0.21	0.47 ± 0.20	0.51 ± 0.19	0.52 ± 0.20	0.57 ± 0.20	0.58 ± 0.21	0.049 <sup>†</sup>	0.001 <sup>†</sup>
phase cross-correl. $\tau_0$	Control	2.0 ± 2.0	2.0 ± 1.7	2.2 ± 1.3	2.5 ± 1.5	2.0 ± 0.9	2.0 ± 0.9	2.6 ± 1.5	2.6 ± 1.5	0.6*	0.7*
	Stroke	6.6 ± 6.7	5.9 ± 5.3	3.8 ± 3.4	3.6 ± 3.5	5.3 ± 5.6	5.7 ± 5.9	5.9 ± 5.4	5.8 ± 5.6	0.0003 <sup>†</sup>	0.0004 <sup>†</sup>

\* P value between physiologic conditions comparisons

† P value between groups comparisons

TABLE III: The maximum correlation strength  $C_{\max}$  and the characteristic lag  $\tau_0$  obtained from the direct cross-correlation of the BP and BFV signals and from the cross-correlation of the instantaneous phase increments in the BP and BFV signals, as well as the entropy index  $\rho$  obtained from the synchronization analysis for the control and stroke group during different physiologic conditions. We compare data from BFV in the right MCA (BFV-MCAR) in healthy subjects with data from BFV in the normal side MCA in post-stroke subjects (mean ± standard deviation values are presented in the left column for each condition). We compare data from BFV in the left MCA (BFV-MCAL) in healthy subjects with data from BFV in the stroke side MCA in post-stroke subjects (mean ± standard deviation values are presented in the right column for each condition). The p values from 2x4 MANOVA are calculated for comparing groups and conditions difference.

maximum of  $|C(\tau)|$  during each heart beat period along both positive and negative lags, and find two points in those maxima with largest time lags at which the correlation are still above  $rC_{\max}$ . The average of absolute values of these two points gives the characteristic time lags  $\tau_0$ . From  $\tau_0$  and  $C_{\max}$  for all subjects and during all physiologic conditions, one can confirm that the stroke group tends to have larger  $C_{\max}$  and longer time lag  $\tau_0$  compared to those for the control group.

We apply MANOVA to demonstrate whether  $\tau_0$  and  $C_{\max}$  are different for healthy and post-stroke subjects. The results are shown in Table III. We find that during tilt and hyperventilation, the control and stroke groups are not significantly different (p values > 0.05). In contrast, during supine rest and CO<sub>2</sub> re-breathing, the difference between the control group and the stroke group becomes significant (p values < 0.05).

To explain the above difference in  $\tau_0$  and  $C_{\max}$  during supine rest, we note that post-stroke subjects exhibit higher BP and CO<sub>2</sub> mean values in baseline (see Table I). Therefore, the BP-BFV autoregulatory curve for post-stroke subjects is shifted to the right, to higher BP values, while at the same time the plateau of this curve is narrowed due to the higher level of CO<sub>2</sub> [3]. CO<sub>2</sub> rebreathing increases the level of the CO<sub>2</sub> after the period of hyperventilation (hypocapnia), thus further testing the reactivity of the CA which shows impaired vasodilatory responses in post-stroke subjects. In contrast, vasoconstrictor responses to tilt-up hyperventilation are preserved.

#### IV. DISCUSSION AND CONCLUSIONS

In this study we investigate dynamics of cerebral autoregulation from the relationship between the peripheral BP in the finger and the cerebral BFV for a group of healthy and post-stroke subjects during the four different physiologic conditions of supine, tilt, hyperventilation, CO<sub>2</sub> rebreathing. The mechanism of cerebral autoregulation is traditionally accessed through the response of the average cerebral BFV to abrupt perturbation in the the average BP (e.g., upright tilt from supine position), and is typically characterized by the ability of the cerebral blood vessels to restore equilibrium and a steady cerebral blood flow after such perturbation — a process which is known to operate on time scales above several heartbeats. In contrast, we focus on the dynamical characteristics of the pressure-flow fluctuation around average values. We show that in healthy subjects the CA mechanism is active even during the steady equilibrium state. Moreover, we find that on top of the BFV waveforms associated each heartbeat there are robust fluctuations which are reduced in the post-stroke subjects, indicating an active cerebral vascular regulation in healthy subjects on time scales within a single heartbeat even under steady BP.

To test for the dynamical patterns in the BP-BFV fluctuations we use four different methods, and we compare the results of the analyses by evaluating the combined effects of pressure autoregulation (upright tilt) and metabolic autoregulation (hyperventilation and CO<sub>2</sub> rebreathing) in healthy and post-stroke subjects. We find

that the gain and phase obtained from the traditional transfer function analysis do not provide a significant difference between healthy and post-stroke subjects. In contrast, the coherence is significantly different in the heartbeat frequency range (0.7-1.4 Hz) when we compare both the normal side and the stroke side of post-stroke subjects with healthy subjects.

Further, we find that the amplitude of the direct cross-correlation between the BP and BFV signals does not separate the control from the stroke group and between different physiologic conditions when we compare the normal side of post-stroke subjects with healthy subjects. However, comparing the stroke side of post-stroke subjects with healthy subjects, we find a statistically significant difference, suggesting that direct cross-correlation method is sensitive to detect abnormalities in CA only for the stroke side. In addition, we observe a significantly faster decay in the BP-BFV cross-correlation function for healthy subjects, reflecting higher beat-to-beat variability in the BP and BFV signals, compared to post-stroke subjects.

Since both BP and BFV are driven by the heartbeat, we also test the coupling between these two signals applying the phase synchronization method. For healthy subjects we observe a weaker synchronization between BP and BFV characterized by lower value of the synchronization index  $\rho$  compared to post-stroke subjects, indicating that the CA mechanism modulates the cerebral BFV waves so that they are not completely synchronized with peripheral BP waves driven by the heartbeat. We find a significantly stronger BP-BFV synchronization in post-stroke subjects associated with loss of cerebral autoregulation.

To probe how the CA mechanism modulates the BFV we investigate the dynamical patterns in the instantaneous phase increments of the BP signals  $\Delta\varphi_{BP}$  and compare them with the patterns we find in the instantaneous phase increments of the BFV signals  $\Delta\varphi_{BFV}$ . Remarkably, we find that for post-stroke subjects  $\Delta\varphi_{BP}$  and  $\Delta\varphi_{BFV}$  exhibit practically identical patterns in time, leading to very high degree of cross-correlation between

$\Delta\varphi_{BP}$  and  $\Delta\varphi_{BFV}$ . In contrast, for healthy subjects  $\Delta\varphi_{BFV}$  exhibits robust random fluctuations very different from the structured oscillatory patterns we find in  $\Delta\varphi_{BP}$ . This leads to a significantly reduced cross-correlation between  $\Delta\varphi_{BP}$  and  $\Delta\varphi_{BFV}$  for healthy subjects compared to post-stroke subjects. Our results indicate a statistically significant separation between the stroke and the control group when we compare both the normal and the stroke side in post-stroke subjects with healthy subjects. This suggests that our new approach based on cross-correlation of the instantaneous phase increments of BP and BFV is sensitive to detect impairment of cerebral vascular autoregulation in both hemispheres for subjects with minor ischemic stroke.

Our findings of robust fluctuations in  $\Delta\varphi_{BFV}$ , which do not synchronize with periodic patterns in  $\Delta\varphi_{BP}$ , clearly indicate that the mechanism of cerebral autoregulation impacts the dynamics not only on scales above several heartbeats but is also active within a single heartbeat, i.e., much shorter time scales than previous known. Since these fluctuations are present in the data after we have truncated the a part of BP and BFV signals corresponding to the initial perturbation related to changes in the physiologic condition, our results also suggest that the cerebral autoregulation plays an important role even in the quasi-steady state.

### Acknowledgments

Z.C., K.H., H.E.S., and P.Ch.I. acknowledge support from NIH Grant No. HL071972, No. 2R01 HL071972 and NIH/National Center for Research Resources Grant No. P41RR13622. V.N. acknowledges support from CIMIT - New Concept grant (W81XWH), American Heart Foundation Grant No. 99 30119N, 1R01 NIH-NINDS (1R01-NS045745-01), NIH GCRC Grant 5 MOIRR00034 and MO1-RR01302, and The Older American Independence Center Grant 2P60 AG08812-11.

- 
- [1] N. A. Lassen, *Physiol. Rev.* **39**, 183 (1959).
  - [2] K. Narayanan, J. J. Collins, J. Hamner, S. Mukai, and L.A. Lipsitz, *Am. J. Physiol. Regulatory Integrative Comp. Physiol.* **281**, R716 (2001).
  - [3] R. B. Panerai, *Physiol. Meas.* **19**, 305 (1998).
  - [4] S. Schwarz, D. Georgiadis, A. Aschoff, and S. Schwab, *Stroke* **33**, 497 (2002).
  - [5] P. J. Eames, M. J. Blake, S. L. Dawson, R. B. Panerai, and J. F. Potter, *J. Neurol. Neurosur. Ps.* **72**, 467 (2002).
  - [6] V. Novak, A. Chowdhary, B. Farrar, H. Nagaraja, J. Braun, R. Kanard, P. Novak, and A. Slivka, *Neurology* **60**, 1657 (2003).
  - [7] V. Novak, A. C. Yang, L. Lepicovsky, A. L. Goldberger, L. A. Lipsitz, and C.-K. Peng, *BioMedical Engineering online* **3**, 39 (2004).
  - [8] S. S. Kety, and C. F. Schmidt, *J. Clin. Invest.* **29**, 476 (1948).
  - [9] W. D. Obrist, H. K. Thompson, H. S. Wang, and W. E. Wilkinson, *Stroke* **6**, 245 (1975).
  - [10] R. Aaslid, K. F. Lindegaard, W. Sorteberg, and H. Nornes, *Stroke* **20**, 45 (1989).
  - [11] F. P. Tiecks, A. M. Lam, R. Aaslid, and D. W. Newell, *Stroke* **26**, 1014 (1995).
  - [12] S. L. Dawson, M. J. Blake, R. B. Panerai, and J. F. Potter, *Cerebrovasc. Dis.* **10**, 126 (2000).
  - [13] R. B. Panerai, S. L. Dawson, and J. F. Potter, *Am. J. Physiol. Heart Circ. Physiol.* **277**, H1089 (1999).
  - [14] R. B. Panerai, S. L. Dawson, P. J. Eames, and J. F. Potter, *Am. J. Physiol. Heart Circ. Physiol.* **280**, H2162 (2001).

- [15] P. Ch. Ivanov, M. G. Rosenblum, C.-K. Peng, J. Mietus, S. Havlin, H. E. Stanley, and A. L. Goldberger, *Nature* **383**, 6598 (1996).
- [16] S. Havlin, L. A. N. Amaral, Y. Ashkenazy, A. L. Goldberger, P. Ch. Ivanov, C.-K. Peng, and H. E. Stanley, *Physica A* **274**, 99 (1999).
- [17] P. Ch. Ivanov, L. A. N. Amaral, A. L. Goldberger, S. Havlin, M. G. Rosenblum, H. E. Stanley, and Z. R. Struzik, *Chaos* **11**, 641 (2001).
- [18] A. L. Goldberger, L. A. N. Amaral, J. M. Hausdorff, P. Ch. Ivanov, C.-K. Peng, and H. E. Stanley, *Proc. Natl. Acad. Sci. U.S.A.* **99**, 2466 (2001).
- [19] P. Bernaola-Galvan, P. Ch. Ivanov, L. A. N. Amaral, and H. E. Stanley, *Phys. Rev. Lett.* **87**, 168105 (2001).
- [20] M. Meyer, and O. Stiedl, *Euro. J. Appl. Physiol.* **90**, 305 (2003).
- [21] P. Ch. Ivanov, Z. Chen, K. Hu, and H. E. Stanley, *Physica A* **344**, 685 (2004).
- [22] A. N. Pavlov, A. R. Ziganshin, and O. A. Klimova, *Chaos Solitons Fract* **24**, 57 (2005).
- [23] B. Suki, A. L. Barabasi, Z. Hantos, F. Petak, and H. E. Stanley, *Nature* **368**, 615 (1994).
- [24] A. M. Alencar, S. V. Buldyrev, A. Majumdar, H. E. Stanley, and Suki, *Phys. Rev. Lett.* **87**, 088101 (2001).
- [25] B. Suki, A. M. Alencar, U. Frey, P. Ch. Ivanov, S. V. Buldyrev, A. Majumdar, H. E. Stanley, C. A. Dawson, G. S. Krenz, and M. Mishima, *Fluc. Noise Lett.* **3**, R1 (2003).
- [26] W. A. C. Mutch, M. R. Graham, L. G. Girling, and J. F. Brewster, *Resp. Res.* **6**, 41 (2005).
- [27] B. J. West, L. A. Griffin, H. J. Frederick, and R. E. Moon, *Resp. Physiol. Neurobi.* **145**, 219 (2005).
- [28] J. M. Hausdorff, P. L. Purdon, C.-K. Peng, Z. Ladin, J. Y. Wei, and A. L. Goldberger, *J. Appl. Physiol.* **80**, 1448 (1996).
- [29] J. M. Hausdorff, Y. Ashkenazy, C.-K. Peng, P. Ch. Ivanov, H. E. Stanley, and A. L. Goldberger, *Physica A* **302**, 138 (2001).
- [30] Y. Ashkenazy, J. A. Hausdorff, P. Ch. Ivanov, and H. E. Stanley, *Physica A* **316**, 662 (2002).
- [31] N. Scafetta, L. Griffin, B. J. West, *Physica A* **328**, 561 (2003).
- [32] K. Hu, P. Ch. Ivanov, Z. Chen, M. F. Hilton, H. E. Stanley, and S. A. Shea, *Physica A* **337**, 307 (2004).
- [33] P. Ch. Ivanov, J. M. Hausdorff, S. Havlin, L. A. N. Amaral, K. Arai, V. Schulte-Frohlinde, M. Yoneyama, and H. E. Stanley, *arXiv:cond-mat/0409545* (2004).
- [34] B. J. West, M. Latka, M. Glaubic-Latka, and D. Latka, *Physica A* **318**, 453 (2003).
- [35] I. H. Song, and D. S. Lee, *Lect. Notes. Comput. Sc.* **3561**, 195 (2005).
- [36] M. Bachmann, J. Kalda, J. Lass, V. Tuulik, M. Sakki, and H. Hinrikus, *Med. Biol. Eng. Comput.* **43**, 142 (2005).
- [37] R. Karasik, N. Sapir, Y. Ashkenazy, P. Ch. Ivanov, I. Dvir, P. Lavie, and S. Havlin, *Phys. Rev. E* **66**, 062902 (2002).
- [38] M. Martinis, A. Knezevic, G. Krstacic, and E. Vargovic, *Phys. Rev. E* **70**, 012903 (2004).
- [39] P. Ch. Ivanov, A. Bunde, L. A. N. Amaral, S. Havlin, J. Fritsch-Yelle, R. M. Baevsky, H. E. Stanley, and A. L. Goldberger, *Europhys. Lett.* **48**, 594 (1999).
- [40] A. Bunde, S. Havlin, J. W. Kantelhardt, T. Penzel, J. H. Peter, and K. Voigt, *Phys. Rev. Lett.* **85**, 3736 (2000).
- [41] J. W. Kantelhardt, Y. Ashkenazy, P. Ch. Ivanov, A. Bunde, S. Havlin, T. Penzel, J. H. Peter, and H. E. Stanley, *Phys. Rev. E* **65**, 051908 (2002).
- [42] A. Dudkowska and D. Makowiec, *Physica A* **336**, 174 (2004).
- [43] M. Staudacher, S. Telsler, A. Amann, H. Hinterhuber, and M. Ritsch-Martel, *Physica A* **349**, 582 (2005).
- [44] K. Hu, P. Ch. Ivanov, M. F. Hilton, Z. Chen, R. T. Ayers, H. E. Stanley, and S. A. Shea, *Proc. Natl. Acad. Sci. U.S.A.* **101**, 18223 (2004).
- [45] C. Hugenii, *Horoloquim Oscilatorium* (Parisiis, France, 1673).
- [46] V. S. Anischenko, T. E. Vadivasova, D. E. Postnov, and M. A. Safonova, *Int. J. Bifurcation Chaos Appl. Sci. Eng.* **2**, 633 (1992).
- [47] L. Fabiny, P. Colet, R. Roy, and D. Lenstra, *Phys. Rev. A* **47**, 4287 (1993); R. Roy, and K. S. Thornburg, *Phys. Rev. Lett.* **72**, 2009 (1994).
- [48] J. F. Heagy, T. L. Carroll, and L. M. Pecora, *Phys. Rev. E* **50**, 1874 (1994).
- [49] I. Schreiber, and M. Marek, *Physica (Amsterdam)* **5D**, 258 (1982); S. K. Han, C. Kurrer, and Y. Kuramoto, *Phys. Rev. Lett.* **75**, 3190 (1995).
- [50] S. Bahar, A. Neiman, L. A. Wilkens, and F. Moss, *Phys. Rev. E* **65**, 050901 (R) (2002).
- [51] D. Rybski, S. Havlin, and A. Bunde, *Physica A* **320**, 601 (2003).
- [52] S. Bahar and F. Moss, *Chaos* **13**, 138 (2003).
- [53] A. S. Pikovsky, *Radiophys. Quantum Electron.* **27**, 576 (1984).
- [54] Y. Kuznetsov, P. Landa, A. Ol'khovoi, and S. Perminov, *Sov. Phys. Dokl.* **30**, 221 (1985).
- [55] M. G. Rosenblum, A. S. Pikovsky, and J. Kurths, *Phys. Rev. Lett.* **76**, 1804 (1996).
- [56] M. G. Rosenblum, A. S. Pikovsky, and J. Kurths, *Phys. Rev. Lett.* **78**, 4193 (1997).
- [57] U. Parlitz, L. Junge, W. Lauterborn, and L. Kocarev, *Phys. Rev. E* **54**, 2115 (1996).
- [58] S. Bahar, *Fluc. Noise Lett.* **4**, L87 (2004).
- [59] A. S. Pikovsky, M. G. Rosenblum, and J. Kurths, *Synchronization: A Universal Concept in Nonlinear Sciences* (Cambridge University Press, Cambridge, 2001).
- [60] S. Boccaletti, J. Kurths, G. Osipov, D. L. Valladares, and C. S. Zhou, *Phys. Rep.* **366**, 1 (2002).
- [61] C. Schafer, M. G. Rosenblum, J. Kurths, H. H. Abel, *Nature (London)* **392**, 239 (1998).
- [62] K. Kotani, I. Hidaka, Y. Yamamoto, and S. Ozono, *Method. Inform. Med.* **39**, 153 (2000).
- [63] M. B. Lotric and A. Stefanovska, *Physica A* **283**, 451 (2000).
- [64] R. Mrowka, A. Patzak, M. G. Rosenblum, *Int. J. Bifur. Chaos* **10**, 2479 (2000).
- [65] A. Stefanovska, H. Haken, P. V. E. McClintock, M. Hozic, F. Bajrovic, and S. Ribaric, *Phys. Rev. Lett.* **85**, 4831 (2000).
- [66] A. Stefanovska and M. Hozic, *Prog. Theor. Phys. Suppl.* **139**, 270 (2000).
- [67] L. Angelini, M. D. Tommaso, M. Guido, K. Hu, P. Ch. Ivanov, D. Marinazzo, G. Nardulli, L. Nitti, M. Pellicoro, C. Pierro, and S. Stramaglia, *Phys. Rev. Lett.* **93**, 038103 (2004).
- [68] P. Tass, M. G. Rosenblum, J. Weule, J. Kurths, A. Pikovsky, J. Volkmann, A. Schnitzler and H.-J. Freund, *Phys. Rev. Lett.* **81**, 3291 (1998).

- [69] F. Nobili, G. Rodriguez, A. Arrigo, B. M. Stubinski, E. Rossi, and R. Cerri et al., *Lupus* **5**, 93 (1996).
- [70] G. Leftheriotis, J. M. Geraud, M. P. Preckel, and J. L. Saumet, *Clin. Physiol.* **15**, 537 (1995).
- [71] H. Sugimori, S. Ibayashi, K. Fujii, S. Sadoshima, Y. Kuwabara Y, and M. Fujishima, *Stroke* **26**, 2053 (1995).
- [72] J. M. Serrador, P. A. Picot, B. K. Rutt, J. K. Shoemaker, and R. L. Bondar, *Stroke* **31**, 1672 (2000).
- [73] J. F. Claerbout, *Fundamentals of Geophysical Data Processing* ( McGraw-Hill, New York, 1976).
- [74] A. V. Oppenheim, and R. W. Schaffer, *Discrete-Time signal Processing, 2nd ed.* (Prentice-Hall, UpperSaddle River, New Jersey, 1998).
- [75] P. Ch. Ivanov, A. L. Goldberger, S. Havlin, C.-K Peng, M. G. Rosenblum, and H. E. Stanley, “*Wavelets in Medicine and Physiology*” in “*Wavelets in Physics*”, editor J. C. van den Berg (Cambridge University Press, Cambridge, 1998).
- [76] S. L. Marple, *IEEE T. Signal Proces.* **47**, 2600 (1999).
- [77] L. Cimponeriu, M. Rosenblum, and A. Pikovsky, *Phys. Rev. E* **70**, 046213 (2004).